



## A POSSIBLE DICHROMATIC NEUTRINO BEAM FOR A 1 TEV ACCELERATOR

Linda Stutte

January 2, 1979

### Introduction

This report summarizes a design study of new dichromatic neutrino beams to extend the range of available energies covered by the existing dichromatic train<sup>1</sup>, once the accelerator achieves Tevatron operation. The existing train can run at secondary hadron momentum below 350 GeV. Its initial targetting angles (with respect to the apparatus) are 11.7 mr (horizontal) and 1.3 mr (vertical). It is important to keep these angles large in order to minimize backgrounds from decays before momentum and sign selection can occur (wide band background). This train has a solid angle acceptance of  $11.5 \Omega$  sr, a reasonable match to particle production spectra in this energy region. One of the drawbacks of this train is its very complicated arrangement of proton beam dumping, using fixed aperture collimators inserted inside magnets to act as beam absorbers. This may lead to a shortened operational lifetime for the train, and certainly contributes to the complexity of tune-up and acceptance studies.

### Design Goals

There were six parameters that were thought to be important at the early stages of the design effort. As is the case in almost any real life situation, one must choose a subset of this idealized set, since in practice, one parameter is usually optimized at the expense of one or more of the others.

This ideal set consisted of the following items:

1. Reach secondary beam momenta up to  $X_F \sim 3/4$   
( $E_{\max} \sim 750$  GeV).
2. Dump the non-interacting fraction of the primary proton beam cleanly, at all secondary momenta, and at a physical distance of less than 175 feet from the target, in order to utilize the existing bathtub for radioactive ground water containment.
3. Reduce the wide band background component of the beam as much as possible (better or at least as good as the existing design).
4. Obtain an energy resolution on individual events observed at the Z location of the 15' bubble chamber (and for radial positions of up to one meter) of  $\frac{\Delta E}{E} \lesssim 10\%$  for all secondary momenta. (This condition implies that the secondary beam divergence should be  $\lesssim 0.05$  mr.).
5. Obtain the highest flux of secondaries possible while keeping the momentum bite of the beam  $\lesssim 10\%$ .
6. Contain the physical size (both longitudinal and transverse dimensions) of the beam layout in order to minimize costs which would result from new construction necessary to house this train.

The motivation for most of the points above is probably clear and needs little further discussion. Item 4 (improved energy resolution) is necessary for a detailed study of charged current structure functions; with the additional constraint of item 3, (low wide band background) one can also hope to obtain structure functions for neutral currents.

The final design is an amalgam of various attempts which sought to optimize different subsets of the above list. Items 1 and 2 were considered essential in every design. This final design emphasizes good energy resolution and small wide band background as the next two most important features that were optimized. Other designs (not discussed

in detail) had higher secondary fluxes, but much worse wide band background and energy resolution.

### The Ideal Dichromatic

As a comparison point, the currents for the existing dichromatic train<sup>1</sup>, N-30, were scaled so that one could run it at 750 GeV. The geometric layout is shown in Figure 1. This train would then have to be made out of superconducting dipoles and quadrupoles, hence its new name here, N-30SC. It should be emphasized that this is still not a viable design, since the primary proton beam would then be dumped inside superconducting magnets, causing them to go normal. Its only use is to provide a point of comparison as to what might be obtained in any realistic designs. All data shown were obtained using the neutrino flux program NUADA<sup>2</sup>, and the charged particle Monte Carlo program DECAY TURTLE<sup>3</sup>. Production spectra used in the calculations were either uniform distributions or from the Stefanski-White parametrization<sup>4</sup>.

### Train D-61G

The geometric layout for the final design, here called D-61G, is given in Figure 3. Table I summarizes element locations and magnetic fields needed for 750 GeV operation. The optics of D-61G is a simple point to parallel focussing system, since, at high energies, a small momentum bite does not contribute greatly to improved energy resolution at the detector, unlike the situation at lower energies. (See Figures 8-10, discussed later in more detail.) Although the initial targetting angles (5.77 mr horizontal and 6.42 mr vertical) are not large, one obtains good wide band rejection since the beam does not aim toward the detector until the final bend.

### Comparisons

Figures 2 and 4 show the 600 GeV neutrino flux spectra for N-30SC and D-61G, respectively. These were obtained using NUADA and the Stefanski-White production spectra parametrization. The low energy background arises primarily from decays close to the target, whereas higher energy backgrounds are produced further from the target. N-30SC, which has a larger initial targetting angle ( $\theta_{o\_TOTAL} = 11.8 \text{ mr}$  opposed to 8.6 mr for D-61G) has less low energy wide band background. D-61G, on the other hand, has less high energy background since the beam is always at a large angle with respect to the apparatus, unlike N-30SC.

The magnets considered in the D-61G design were all 6-3-120 dipoles 4Q120 quadrupoles. Smaller aperture magnets would necessarily reduce the secondary flux. Using the large aperture magnets, the angular acceptance obtained is about 33% of that available. This can be seen by comparing the neutrino total flux spectra from N-30SC (Figure 2) to that for D-61G (Figure 4). It is further tabulated in Table II. This table shows various quantities for each beam, generated under two different assumptions: that of a flat production spectra and then utilizing the Stefanski-White parametrization, with the program DECAY TURTLE. Figures 5 and 6 show, for example, the momentum spectra used for each case. It can be seen from the table that N-30SC has much more angular acceptance in both planes than is actually necessary. D-61G, on the other hand, has too large a vertical acceptance and too small a horizontal acceptance. The difference in neutrino flux between these two trains, then, is largely due to the limited horizontal acceptance for D-61G.

This acceptance can be improved by moving the last quadrupole, ØFDT, closer to the target. Doing so, however, increases the wide band background. This happens because this quadrupole cancels some of the dispersion introduced

by ØEDT. Moving the quad closer reduces its effect so that  $\theta_0$  must be smaller. An asymmetric aperture for this quad is probably a better choice.

Dumping for D-61G is straightforward, as seen in Figure 7. For all secondary momenta, the beam dumps into a single fixed position dump, located about 120 feet from the target. For negative secondary running, the last 2 dipoles of ØUDT must be C type magnets, but that should pose no problem.

Table II gives the final angular divergences of the two beams. At high energies ( $\geq 500$  GeV) the energy resolution at the detectors depend strongly on these divergences. This is illustrated in Figures 8-10 which show the results of a Monte Carlo program<sup>5</sup> for these resolutions as a function of detector radius at various neutrino energies. Superimposed on the graphs are the results obtained with the two beams N-30SC and D-61G using the output of NUADA binned in fine radial bins across a 1 meter detector. Clearly at 400 GeV, the two designs are indistinguishable and well within the design goal of  $\frac{\Delta E}{E} \leq 10\%$ . At  $\geq 600$  GeV, the smaller angular divergence of D-61G is clearly evident.

The transverse dimensions of D-61G are shown in Figure 11, superimposed on an outline of the current decay pipe and target tube locations. The elements are positioned so that the final secondary beam position is centered on the axis of the decay pipe. Clearly, with much effort this beam could be squeezed into a relatively small building. The starting elements are so low, however, that they would be scraping near the bottom of the target tube rails so that special bedplates and transporters would have to be designed and constructed. An alternative arrangement might be to rotate the magnets  $180^\circ$ . The existing track and transporters would be usable; a new higher roof for the target tube would then be necessary.

### Event Rates

For D-61G, at 1000 GeV incident and assuming 600 GeV secondaries, the integrated flux of pion and kaon neutrinos is  $3.99 \times 10^{+4}$  and  $2.13 \times 10^4$  neutrinos/GeV/m<sup>2</sup>/10<sup>13</sup> protons, respectively. Assuming neutrino cross sections of  $\sigma_{\nu} = 0.74 E_{\nu} \times 10^{-38}$  cm<sup>2</sup> nucleon<sup>-1</sup> and 20 tons of neon in the 15' bubble chamber (approximated roughly by a cylinder of 1m radius and 8 foot depth), then one expects the number of interacting pion and kaon neutrinos to be  $1.93 \times 10^{-2}/10^{13}$  protons and  $2.92 \times 10^{-2}/10^{13}$  protons, respectively. Thus for 10<sup>13</sup> protons on target, one gets an event every 20 pix. For the larger mass electronic detectors, (of approximately 400 tons), one expects about 1 event per pulse.

### Targetting

Figure 12 shows a possible scheme for a 1 TeV NeuHall, arranged to target at the appropriate angles and positions for D-61G. As is D-61G, all elements are conventional magnets. The quadrupole magnets were laid out as suggested by other authors<sup>6</sup>, and the bends placed as necessary. It can be seen that room is still available to install beam monitoring instrumentation. NeuHall beam element locations and magnet currents are summarized in Table III.

### Summary

A possible design for a new dichromatic neutrino beam to be used during Tevatron operation is discussed. This train requires a target tube of roughly 400 foot length and 8' cross section. The train can be run up to 750 GeV secondary momentum; proton beam dumping is straightforward at all secondary momenta. Good wide band background rejection is obtained; neutrino energy resolutions at the detector are  $\leq 10\%$ . For 600 GeV neutrino operation, 400 ton detectors should obtain 1 event per 10<sup>13</sup> 1000 GeV protons on target.

# REFERENCES

1. D.Edwards, S.Mori, S.Pruss, '350 GeV/c Dichromatic Neutrino Target Train', TM-661, 1976.
2. D.C.Carey and V.A.White, NUADA, PM0011, 1975.
3. K.L.Brown and Ch.Iselin, DECAY TURTLE, PM0031, 1974.
4. R.Stefanski and H.White, 'Neutrino Flux Distributions', FN-292, 1976.
5. Shigeki Mori, private communication.
6. R.Evans and T.Kirk, 'Transport of Tevatron Energy Primary Proton Beams to Neutrino Area', TM-796, 1978.

TABLE I  
D-61G MAGNET LOCATIONS

<u>ELEMENT</u>	<u>z(')</u>	<u>x<sub>0</sub>(')</u>	<u>y<sub>0</sub>(')</u>	<u>θ<sub>x</sub>(mr)</u>	<u>θ<sub>y</sub>(mr)</u>
Target	0	-0.19	-1.50	5.77	-6.42
½" x ½" x 5' coll.	1.5	-0.17	-1.52	5.77	-6.42
ØUDT-1	8.0	-0.13	-1.56	5.77	-6.42
ØUDT-2	19.5	-0.07	-1.62	5.77	-4.25
ØUDT-3	31.0	0.0	-1.65	5.77	-2.09
ØUDT-4	42.5	0.07	-1.66	5.77	0.08
ØUDT-5	54.0	0.13	-1.65	5.77	2.25
ØUDT-6	65.5	0.20	-1.61	5.77	4.41
10' Beam Dump	118.75	0.50	-1.26	5.77	6.58
ØDDT-1	130.25	0.57	-1.19	5.77	6.58
ØDDT-2	141.75	0.64	-1.12	5.77	6.58
ØEDT-1	153.25	0.71	-1.04	5.77	6.58
ØEDT-2	164.75	0.76	-0.96	3.60	6.58
ØEDT-3	176.25	0.79	-0.89	1.44	6.58
ØEDT-4	187.75	0.79	-0.81	-0.73	6.58
ØEDT-5	199.25	0.77	-0.74	-2.90	6.58
ØEDT-6	210.75	0.72	-0.66	-5.06	6.58
ØFDT	262.0	0.36	-0.32	-7.23	6.58
ØCTP 10' coll.	272.75	0.28	-0.25	-7.23	6.58
ØBDT-1*	283.5	0.20	-0.18	-7.23	6.58
ØBDT-2	295.0	0.13	-0.11	-5.78	5.26
ØBDT-3	306.5	0.07	-0.07	-4.34	3.95
ØBDT-4	318.0	0.03	-0.03	-2.89	2.63
ØBDT-5	329.5	0.01	-0.01	-1.45	1.32
END	339.5	0.0	0.0	0.0	0.0

\*NOTE: Magnets of ØBDT are rotated 42.3° CCW.



TABLE I (cont.)

D-61G

MAGNET CURRENTS AT 750 GEV

<u>ELEMENT</u>	<u>FIELD (KGG)</u>	<u>CURRENT (AMPS)</u>	<u>(type)</u>
ØUDT	17.8	1157.0	(6-3-120)
ØEDT	17.8	1157.0	(6-3-120)
ØBDT*	16.0	1040.0	(6-3-120)
ØDDT	3,7 kg/in	790.4	(4Q120)
ØFDT	3.8 kg/in	811.8	(4Q120)

\*NOTE: Magnets of ØBDT are rotated  $42.3^{\circ}$  CCW.

TABLE II  
COMPARISON OF D-61G AND N-30SC  
PHYSICAL CHARACTERISTICS AT 600 GEV/C

<u>Quantity*</u>	<u>Unit</u>	<u>Train D-61G</u> <u>Spectrum</u>		<u>Train N-30SC</u> <u>Spectrum</u>	
		<u>Flat</u>	<u>S-W<sup>5</sup></u>	<u>Flat</u>	<u>S-W</u>
$\pm\Delta\theta_x$	mr	0.33	0.21	0.94	0.58
$\pm\Delta\theta_y$	mr	1.41	0.56	0.93	0.57
$\pm\Delta p/p$	%	14.33	6.62	9.74	7.22
$\pm xDIV$	mr	0.05	0.03	0.10	0.09
$\pm yDIV$	mr	0.12	0.06	0.15	0.12

\*  $\Delta\theta_x$ ,  $\Delta\theta_y$  are the angular acceptances in the horizontal and vertical planes, respectively.

$\Delta p/p$  is the momentum acceptance.

$xDIV$ ,  $yDIV$  are the final angular divergences of the beam in the horizontal and vertical planes, respectively.

All quantities are R.M.S. half-widths.

TABLE III  
1 TEV NEUHALL FOR D-61G

<u>ELEMENT</u>	<u><math>Z_0</math> (')</u> *	<u><math>X_0</math> (')</u>	<u><math>Y_0</math> (')</u>	<u><math>\theta_x</math> (mr)</u>	<u><math>\theta_y</math> (mr)</u>
MV100-5	3133.41	-0.67	744.53	0.	10.0
MV100-6	3144.41	-0.67	744.63	0.	8.56
MV100-7	3165.4	-0.67	744.78	0.	5.71
MV100-8	3186.4	-0.67	744.87	0.	2.86
ØDN-1	3208.41	-0.67	744.89	0.	0.
ØDN-2	3219.91	-0.67	744.89	0.	0.
ØPN-1	3230.91	-0.67	744.89	0.	0.
ØPN-2	3241.91	-0.67	744.88	0.	-1.28
ØPN-3	3252.91	-0.67	744.85	0.	-2.57
ØPN-4	3263.91	-0.67	744.82	0.	-3.85
ØPN-5	3274.91	-0.67	744.77	0.	-5.14
ØEN-1	3287.16	-0.67	744.71	0.	-6.42
ØEN-2	3298.16	-0.68	744.64	-1.24	-6.42
ØEN-3	3309.16	-0.71	744.57	-2.47	-6.42
ØFN-1	3320.91	-0.74	744.49	-3.71	-6.42
ØFN-2	3332.41	-0.78	744.42	-3.71	-6.42
ØWN-1	3389.91	-0.99	744.05	-3.71	-6.42
ØWN-2	3400.91	-1.02	743.99	-2.35	-6.42
ØWN-3	3411.91	-1.07	743.91	-1.0	-6.42
ØWN-4	3422.91	-1.05	743.84	0.35	-6.42
ØDN2-1	3433.91	-1.03	743.77	1.71	-6.42
ØDN2-2	3444.91	-1.01	743.70	1.71	-6.42
ØWN-5	3455.91	-0.99	743.63	1.71	-6.42
ØWN-6	3466.91	-0.97	743.55	3.06	-6.42
ØWN-7	3477.91	-0.93	743.48	4.42	-6.42
TARGET	3492.53	-0.86	743.39	5.77	-6.42

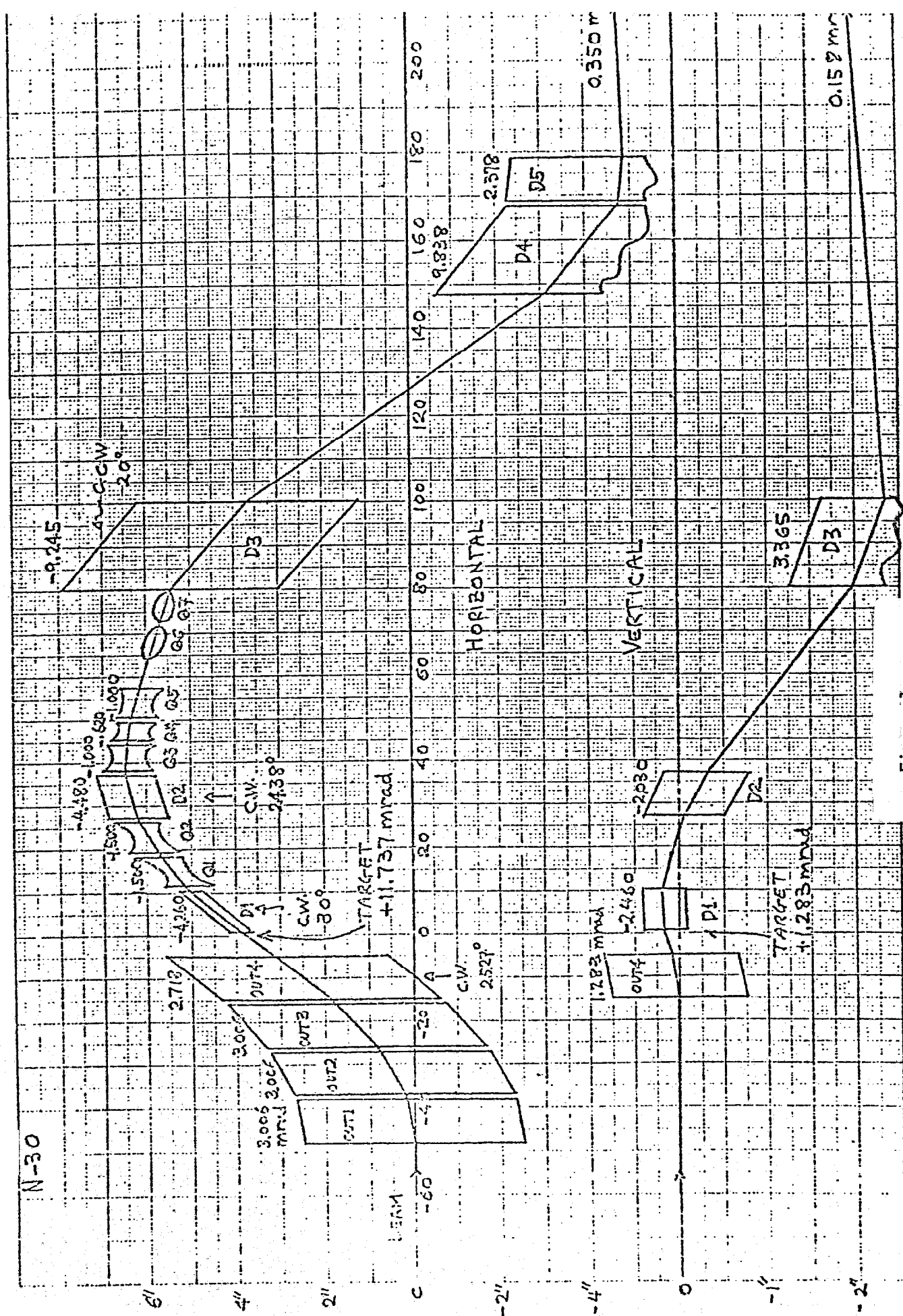
\* NOTE: Coordinates in this table are DUSAF coordinates.  
Table I has relative coordinates.

TABLE III (cont.)  
MAGNET CURRENTS FOR 1 TEV NEUHALL

<u>ELEMENT</u>	<u>FIELD (KG)</u>	<u>CURRENT (AMPS)</u>	<u>(type)</u>
MV100	15.623	4044.8	(4-2-240)
ØDN1	-3.40 kg/in	72.0	(3Q120)
ØPN	14.05	1327.7	(EPB)
ØEN	13.53	1278.6	(EPB)
ØFN	4.70 kg/in	99.6	(3Q120)
ØWN	14.82	1400.5	(EPB)
ØDN2	-3.88 kg/in	82.3	(3Q120)

# FIGURE CAPTIONS

1. Geometric layout of the existing N-30 dichromatic train, used as a model for N-30-SC.
2. Total neutrino flux and right-sign wide band background flux as a function of neutrino energy for train N-30SC tuned to a secondary momentum of 600 GeV/c.
3. Geometric layout of the proposed D-61G dichromatic train.
4. Total neutrino flux and right-sign wide band background flux as a function of neutrino energy for train D-61G tuned to a secondary momentum of 600 GeV/c.
5. Momentum spectrum generated by DECAY TURTLE for flat production spectrum of  $\frac{\Delta p}{p} = \pm 40\%$ .
6. Momentum spectrum generated by DECAY TURTLE using Stefanski-White parametrization for the production spectrum, using  $\frac{\Delta p}{p} = \pm 40\%$ .
7. Optic axis view of primary proton beam trajectory for various secondary momentum settings. Also included on the figure is accepted beam envelope.
8. Observed energy resolution ( $\frac{\Delta E}{E}$  in percent) for kaon neutrinos as a function of detector radius for a detector located at the position of the 15<sup>th</sup> bubble chamber. The curves are generated by a Monte Carlo calculation for an initial kaon neutrino energy of 400 GeV and for various momentum bites and angular divergences, as shown on the figure. Also shown are the results for the trains N-30SC and D-61G.
9. Same as Figure 8, except  $E_K = 600$  GeV.
10. Same as Figure 8, except  $E_K = 750$  GeV.
11. End-on view of D-61G superimposed on an outline of the present target tube and decay pipe. The orientation is chosen so that the final magnetic element is centered on the decay pipe axis.
12. Geometric layout of a possible Neuha11 arrangement of pre-target bends and quadrupoles to satisfy the targetting requirements of D-61G.



## Figure 1

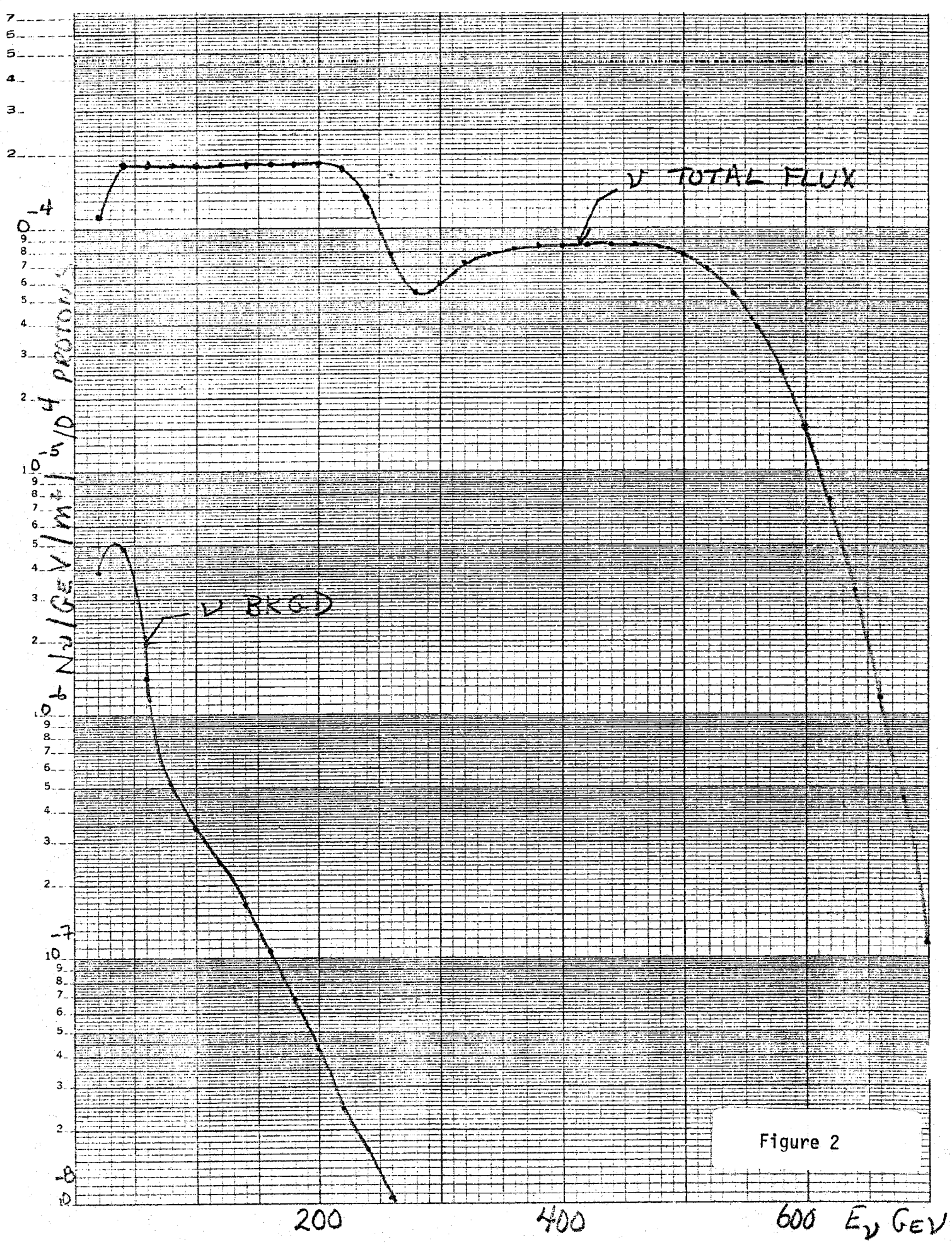


Figure 2

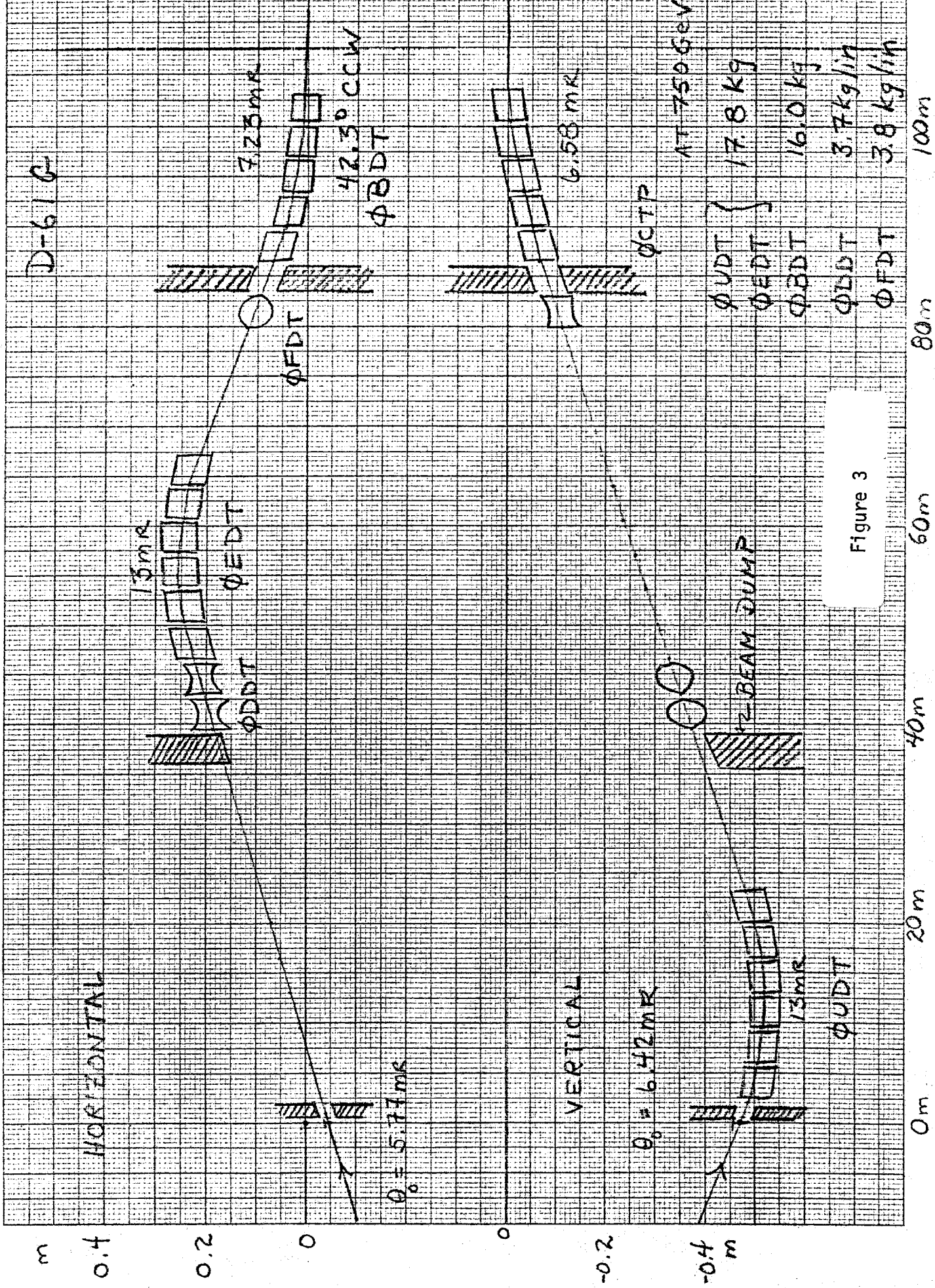


Figure 3



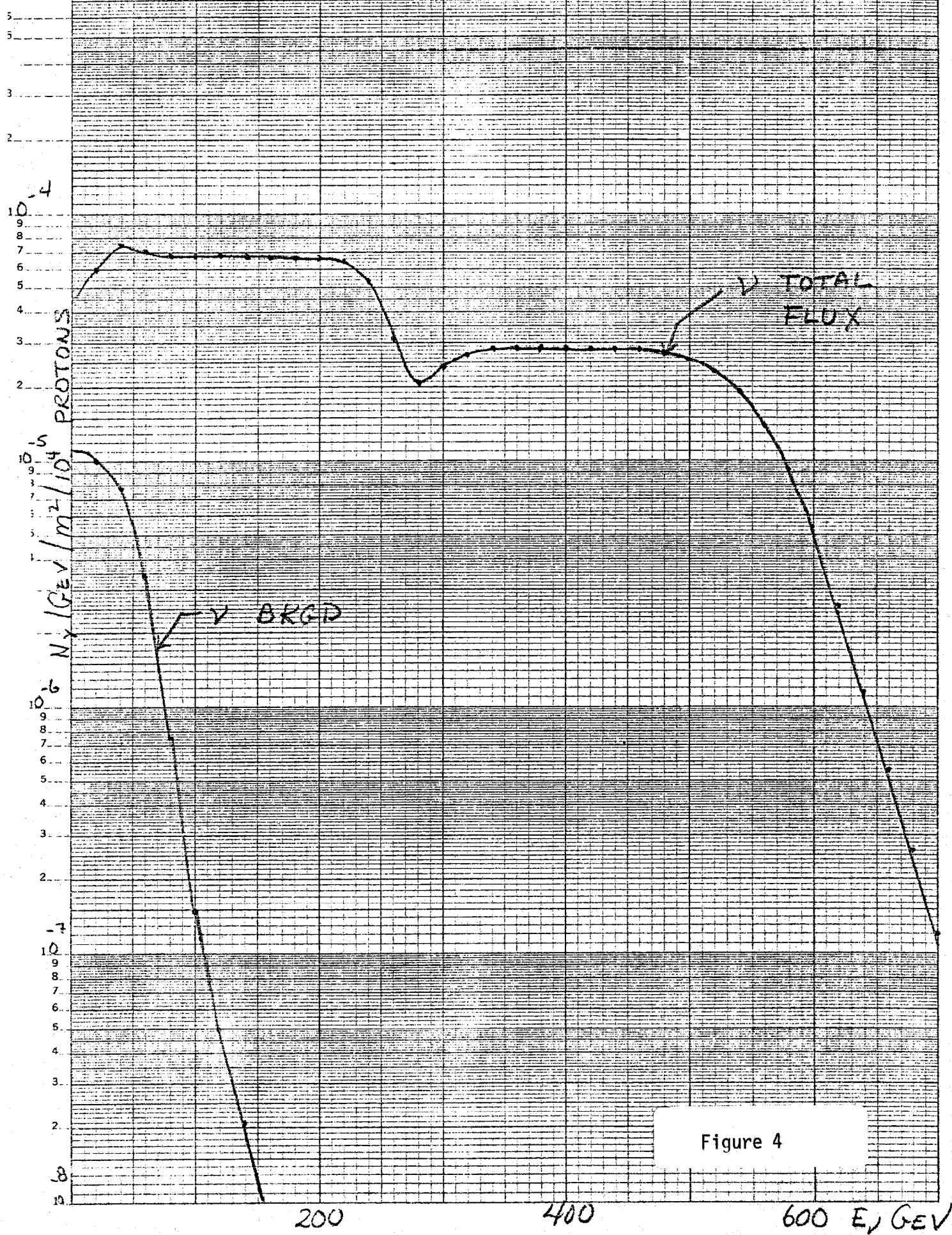


Figure 4

3 1 P TAGEVO

0.006 FT F ON THE TAPSET

SCALE FACTOR.. 100 X'S EQUAL 553 ENTRIES

INTERVAL

0.000

0

25:000

25:000

107:000

107:000

1125:000

1125:000

1175:000

1175:000

2225:000

2225:000

2700:000

2700:000

3350:000

3350:000

3750:000

3750:000

4250:000

4250:000

4750:000

4750:000

5250:000

5250:000

5750:000

5750:000

6250:000

6250:000

6750:000

6750:000

7250:000

7250:000

7750:000

7750:000

8250:000

8250:000

8750:000

8750:000

9250:000

9250:000

9750:000

9750:000

10250:000

10250:000

10750:000

10750:000

11250:000

11250:000

11750:000

11750:000

12250:000

12250:000

12750:000

12750:000

13250:000

13250:000

13750:000

13750:000

14250:000

14250:000

14750:000

14750:000

15250:000

15250:000

15750:000

15750:000

16250:000

16250:000

16750:000

16750:000

17250:000

17250:000

17750:000

17750:000

18250:000

18250:000

18750:000

18750:000

19250:000

19250:000

19750:000

19750:000

20250:000

20250:000

20750:000

20750:000

21250:000

21250:000

21750:000

21750:000

22250:000

22250:000

0

TOTAL NUMBER OF ENTRIES = 10000 INCLUDING UNDERFLOW AND OVERFLOW  
ENTER = 599.862 RMS HALF WIDTH = 138.862

Figure 5

0.000 FT FROM THE TARGET

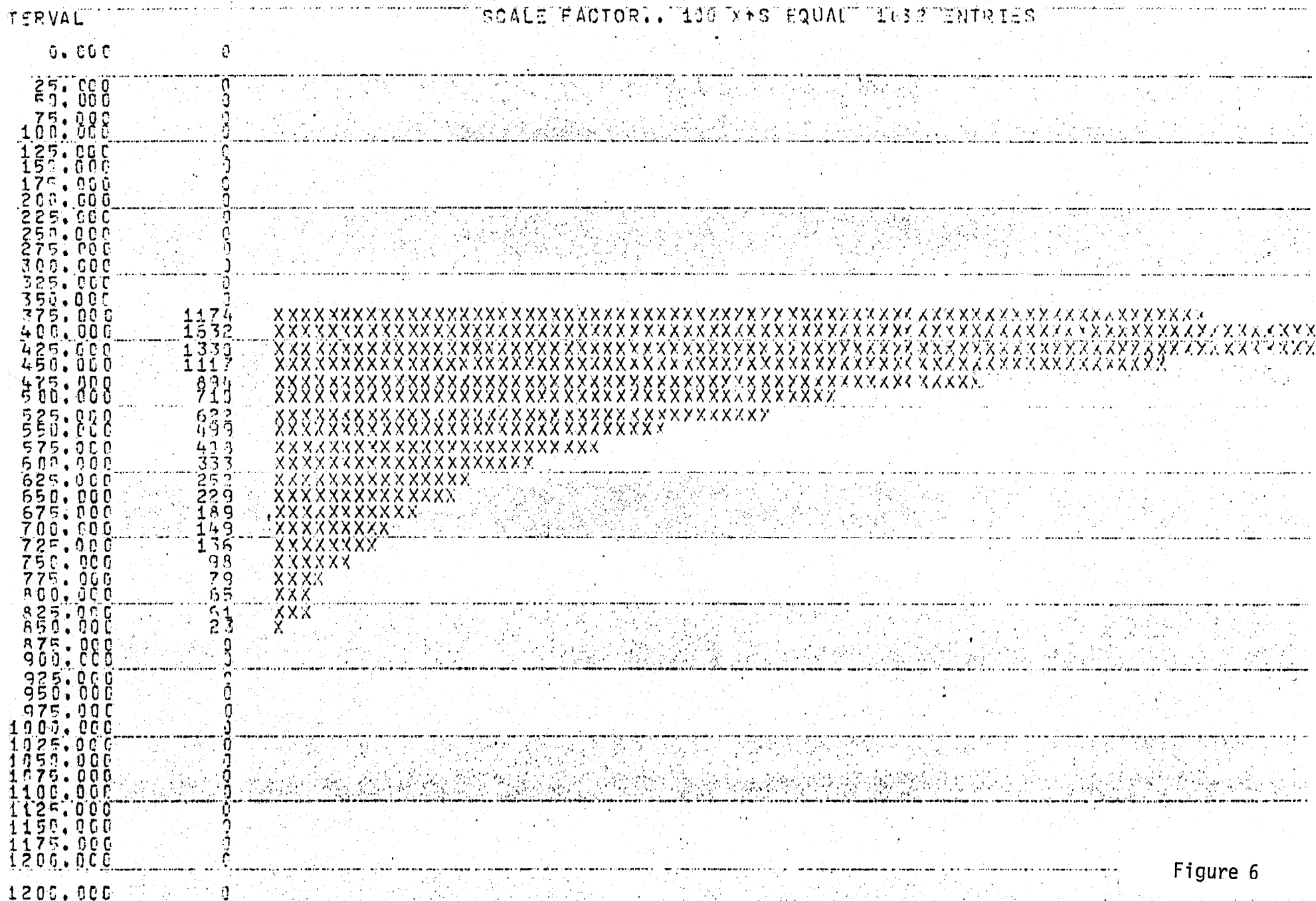
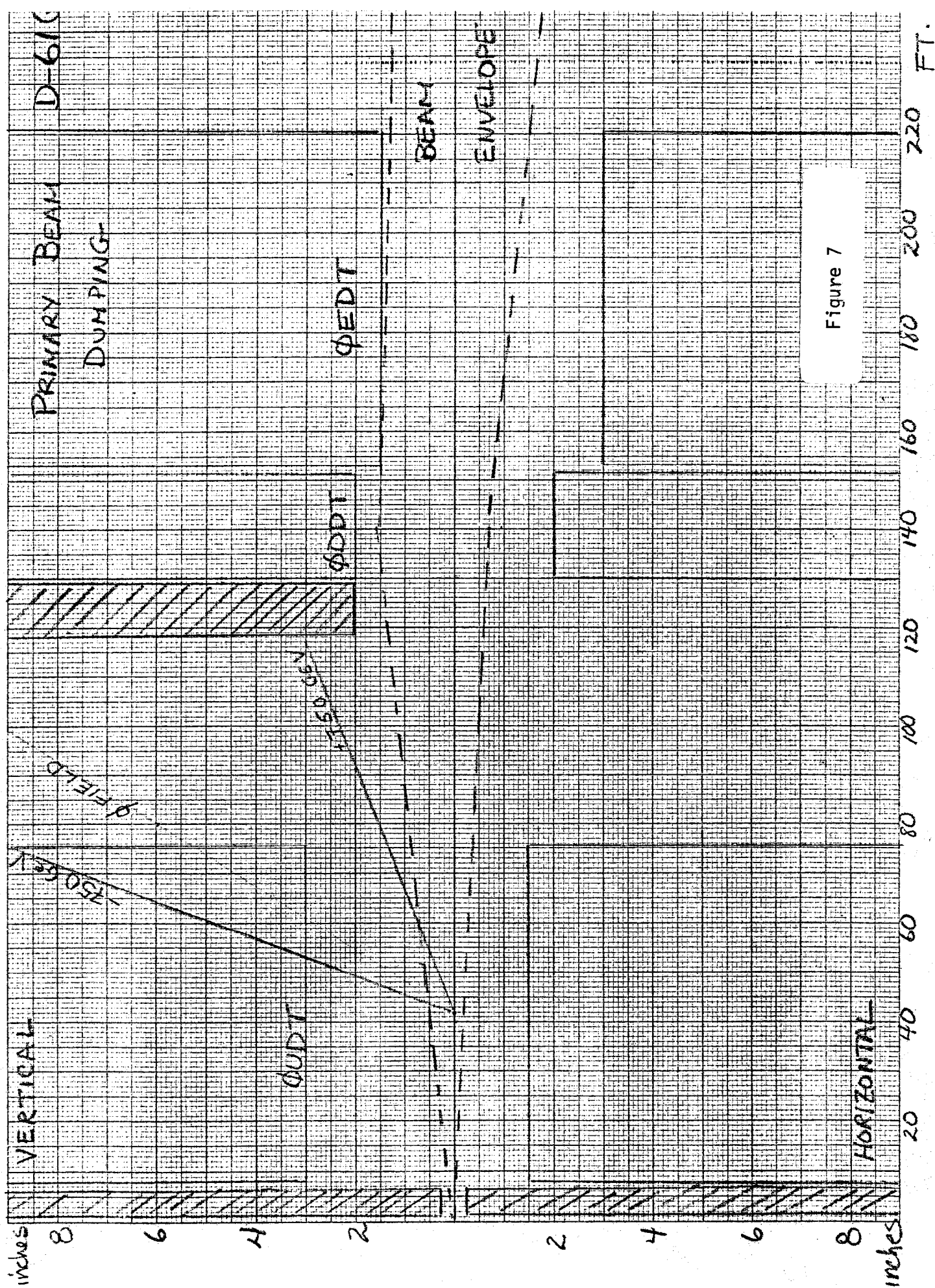


Figure 6

TOTAL NUMBER OF ENTRIES = 10000 INCLUDING UNDERFLOW AND OVERFLOW  
 ITER = 474.681 RMS HALF WIDTH = 102.417



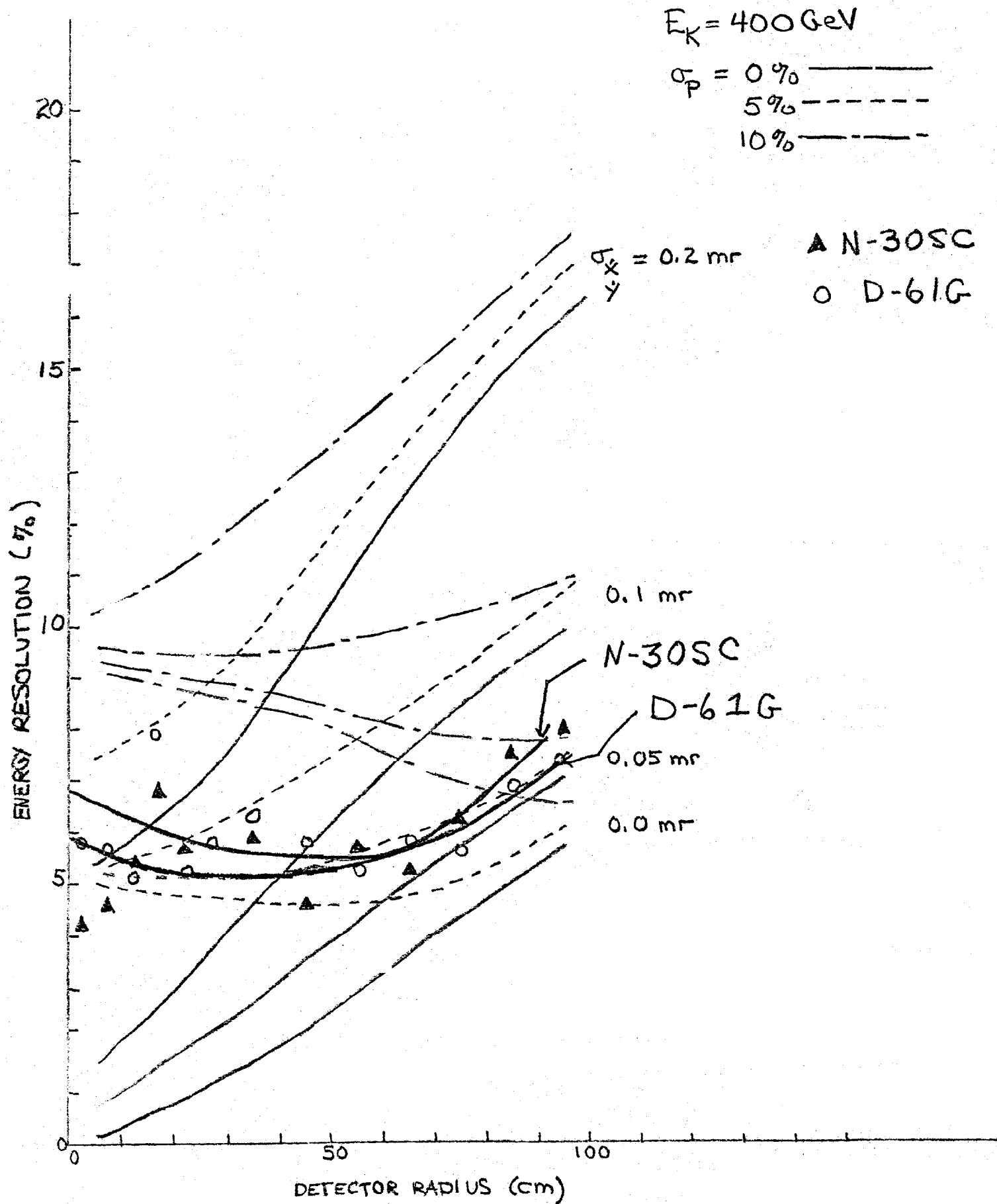


FIGURE 8

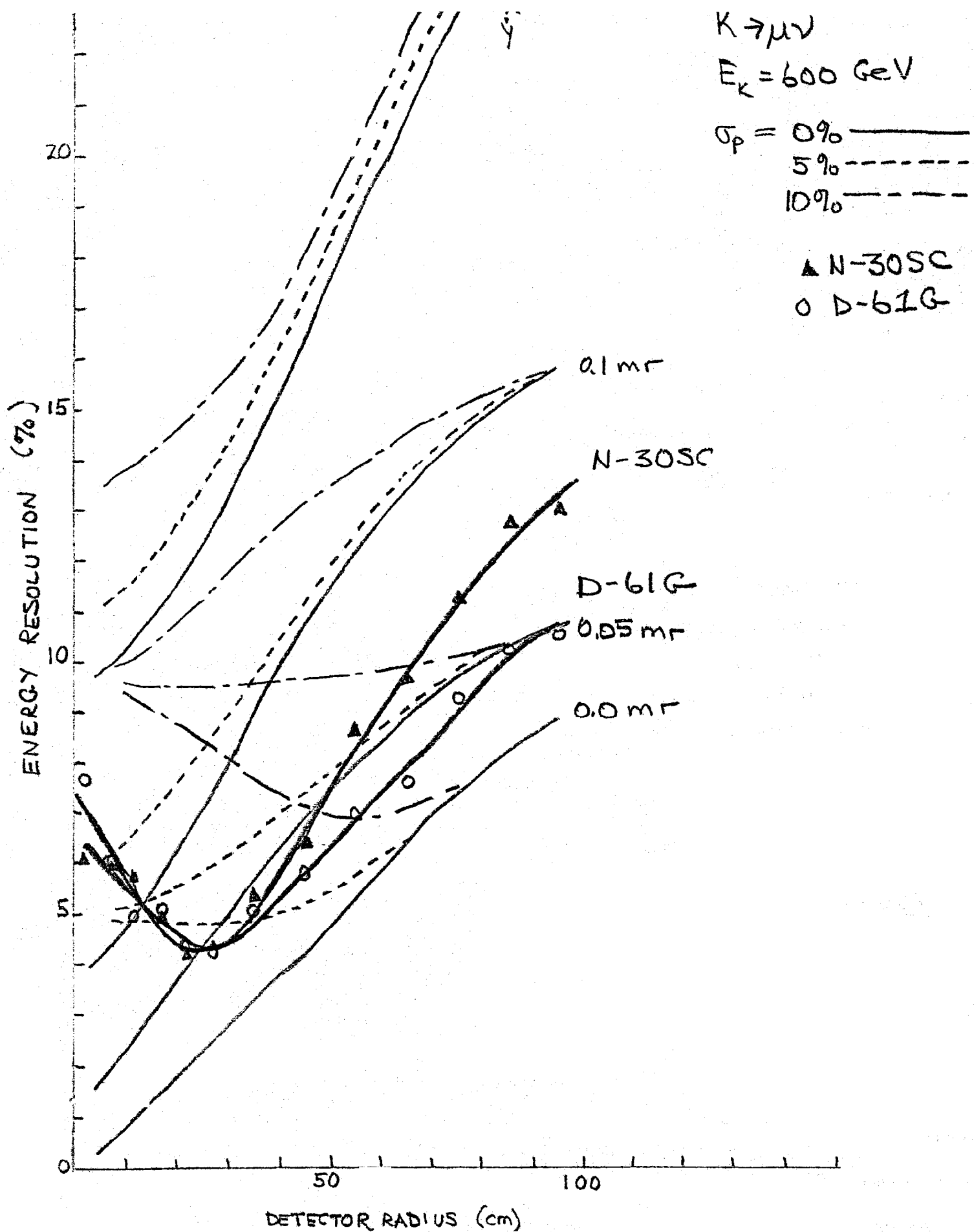


FIGURE 9

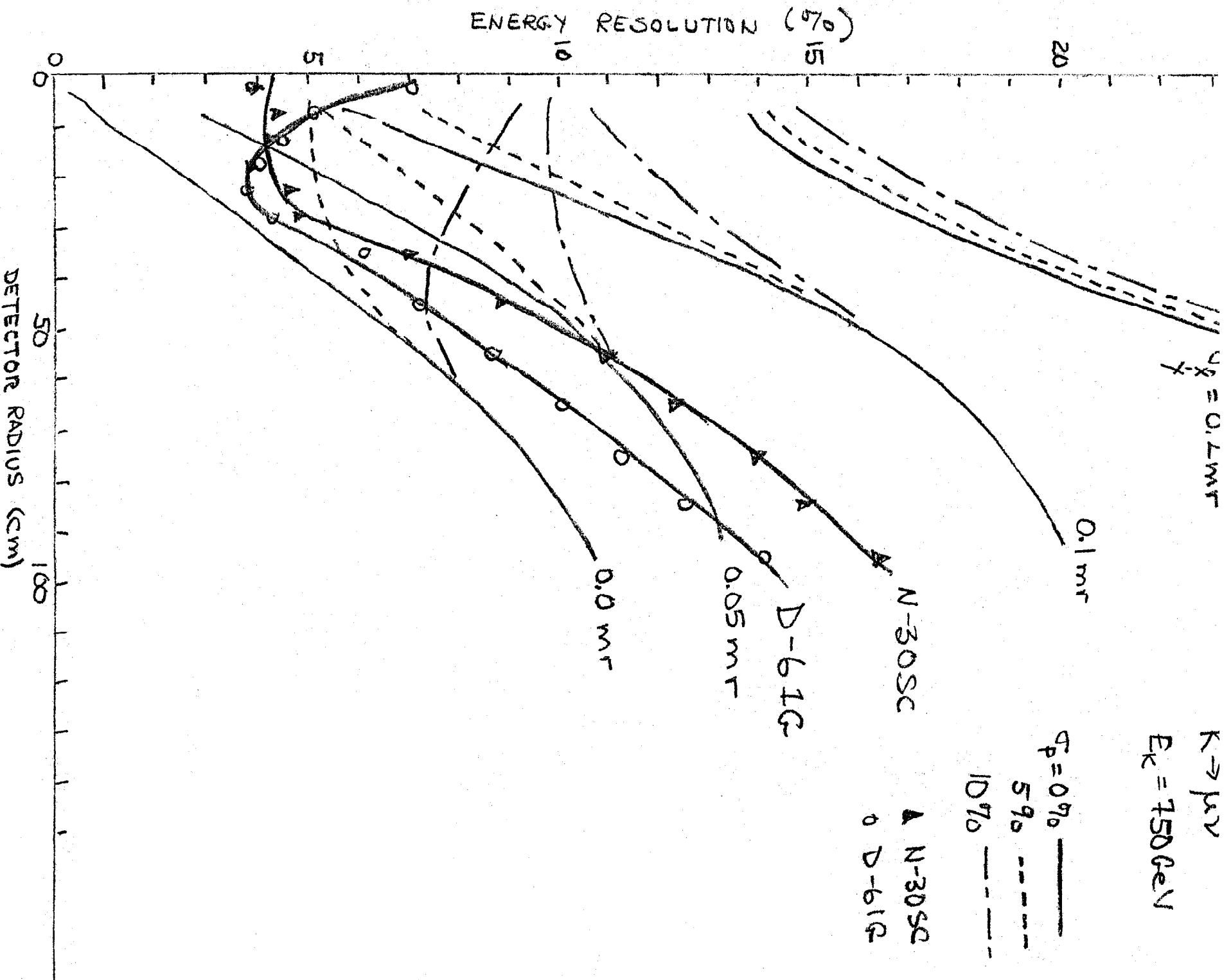


FIGURE 10



# D-61 G END VIEW

$\frac{1}{10}$  SCALE

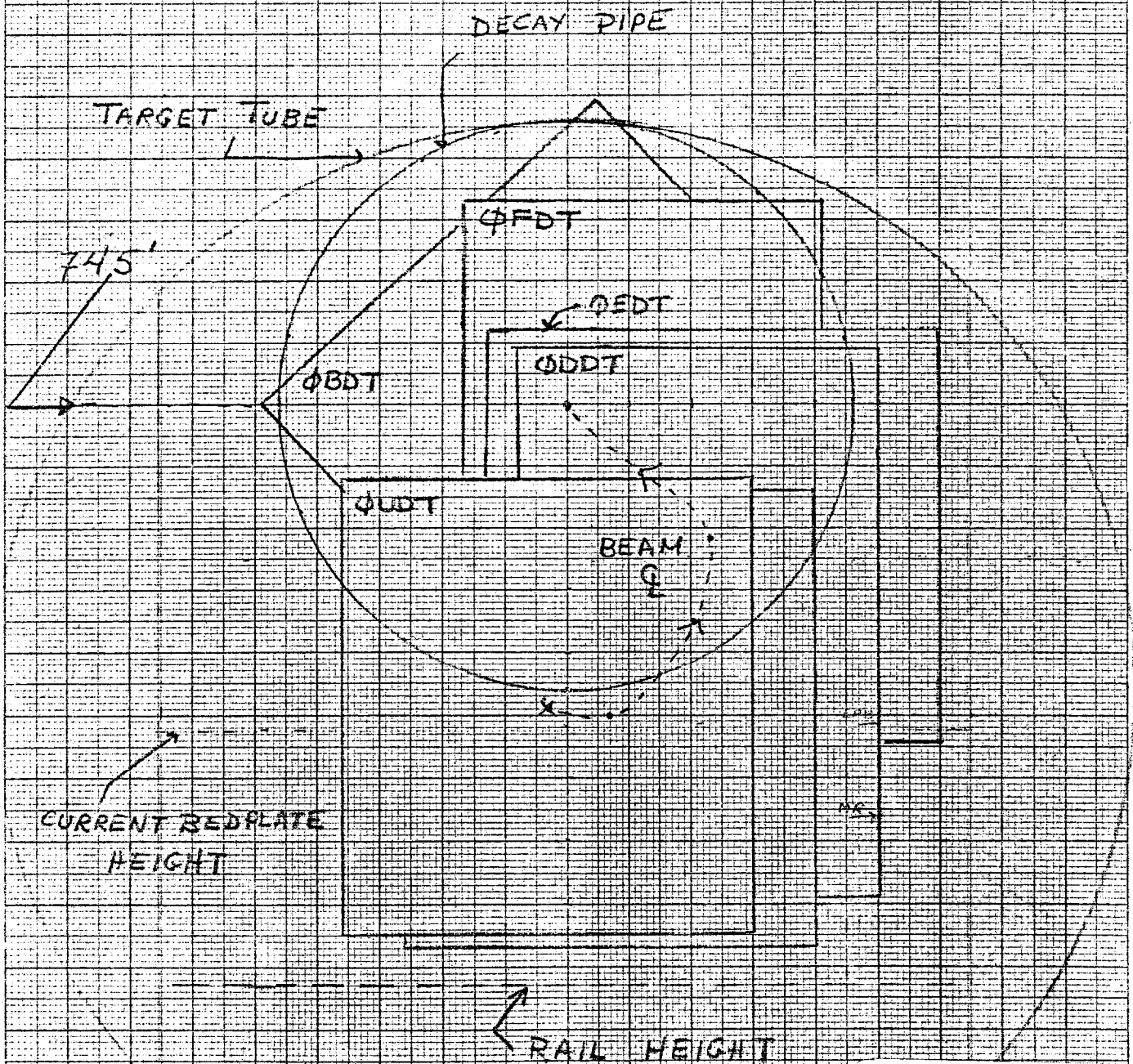
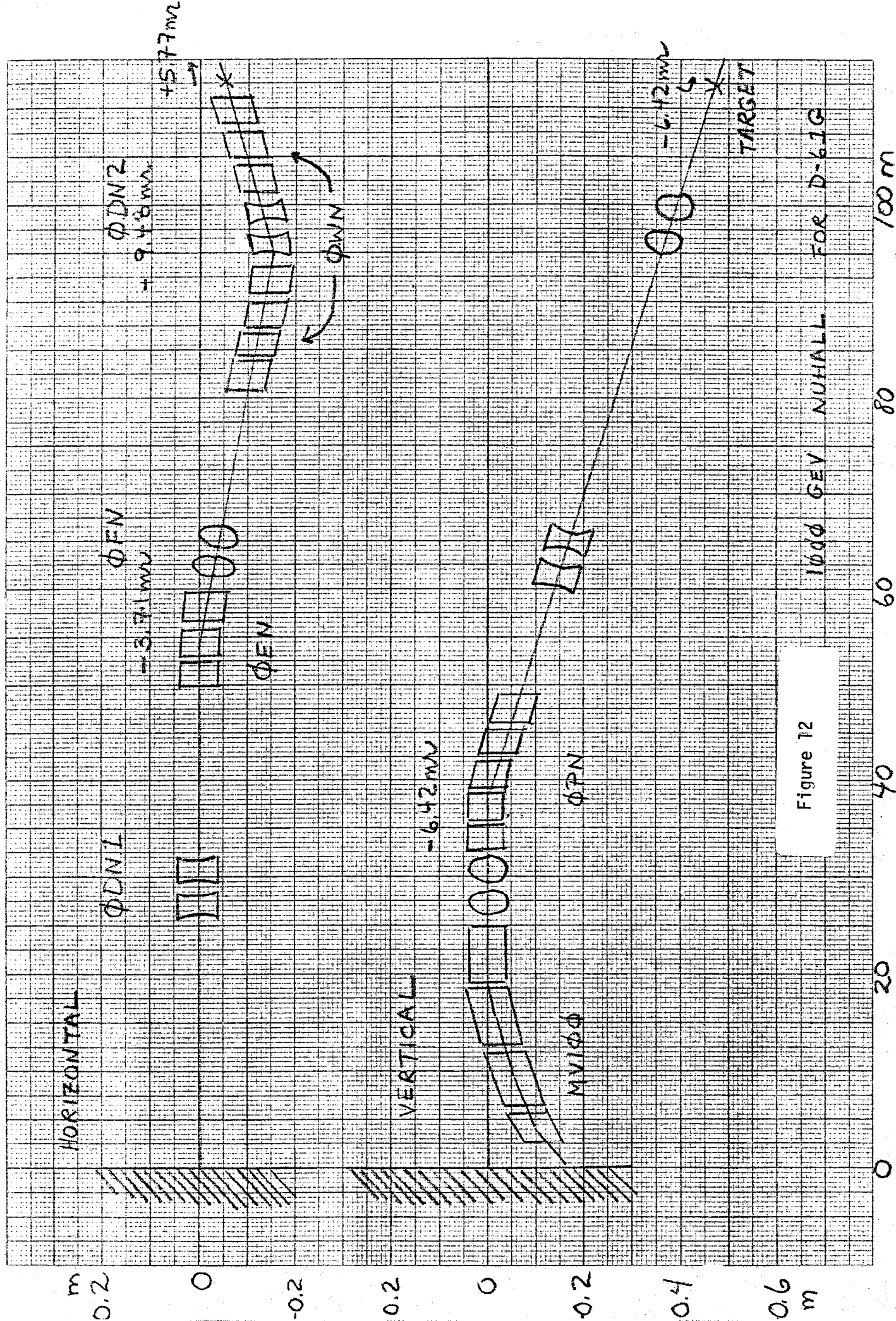


Figure 11





Addendum to

"A Possible Dichromatic Neutrino Beam for a 1 TeV Accelerator"

Linda G. Stutte

January 12, 1980

Current Tevatron construction plans for the Neutrino Area call for an upstream extension of the existing targetting area (Neuhall). The dichromatic train described in TM-841 could then be moved upstream (targetting at  $Z$  location of  $\approx 3000'$ ) and thus provide more neutrino flux due to an increase in decay length. Figure 1 shows a gain in flux of about 40% solely due to this new location. Wide band backgrounds are also reduced slightly ( $\approx 20\%$ ) due to the decreased solid angle of this source viewed at the detector. Also shown in this figure is a further increase in flux (again about 40-50%) achieved by using wider aperture magnets at the end of the train.

In detail, the last quad is replaced by a new quad with a full aperture of 7" in the horizontal and 4" in the vertical; and the final 5 dipoles are opened up from 6-3-120's to 6-5-120's. This last is quite a simple modification to these dipoles<sup>(1)</sup> and should cause no appreciable degradation in their field strength or quality.

The additional flux is achieved by increasing the acceptance in the horizontal plane (where it was reasonably small to begin with). The vertical plane does not change appreciably from the original design. This increase in flux does degrade the angular divergence in the horizontal plane somewhat, but still stays within the necessary

tolerances for good neutrino energy resolution at the detector (Figure 2) and good particle identification of the secondaries<sup>(2)</sup> (Figure 3).

Table I summarizes the resulting beam parameters.

TABLE I

Physical Characteristics of Improved D-61G at 600 GeV/c

Quantity*	Unit	Old D-61G as in TM-841		Larger Aperture Magnets for D-61G	
		Spectrum		Spectrum	
		Flat	S-W <sup>3</sup>	Flat	S-W
$\pm\Delta\theta_x$	mr	0.33	0.21	0.40	0.29
$\pm\Delta\theta_y$	mr	1.41	0.56	1.44	0.59
$\pm\Delta p/p$	%	14.33	6.62	14.33	6.41
$\pm X_{div}$	mr	0.05	0.03	0.07	0.03
$\pm Y_{div}$	mr	0.12	0.06	0.15	0.07

\*  $\Delta\theta_x$ ,  $\Delta\theta_y$  are the angular acceptances in the horizontal and vertical planes, respectively.  $\Delta p/p$  is the momentum acceptance.

$X_{div}$ ,  $Y_{div}$  are the final angular divergences of the beam in the horizontal and vertical planes, respectively.

All quantities are rms half-widths, as calculated by the Monte Carlo program DECAY TURTLE<sup>4</sup>.

#### References

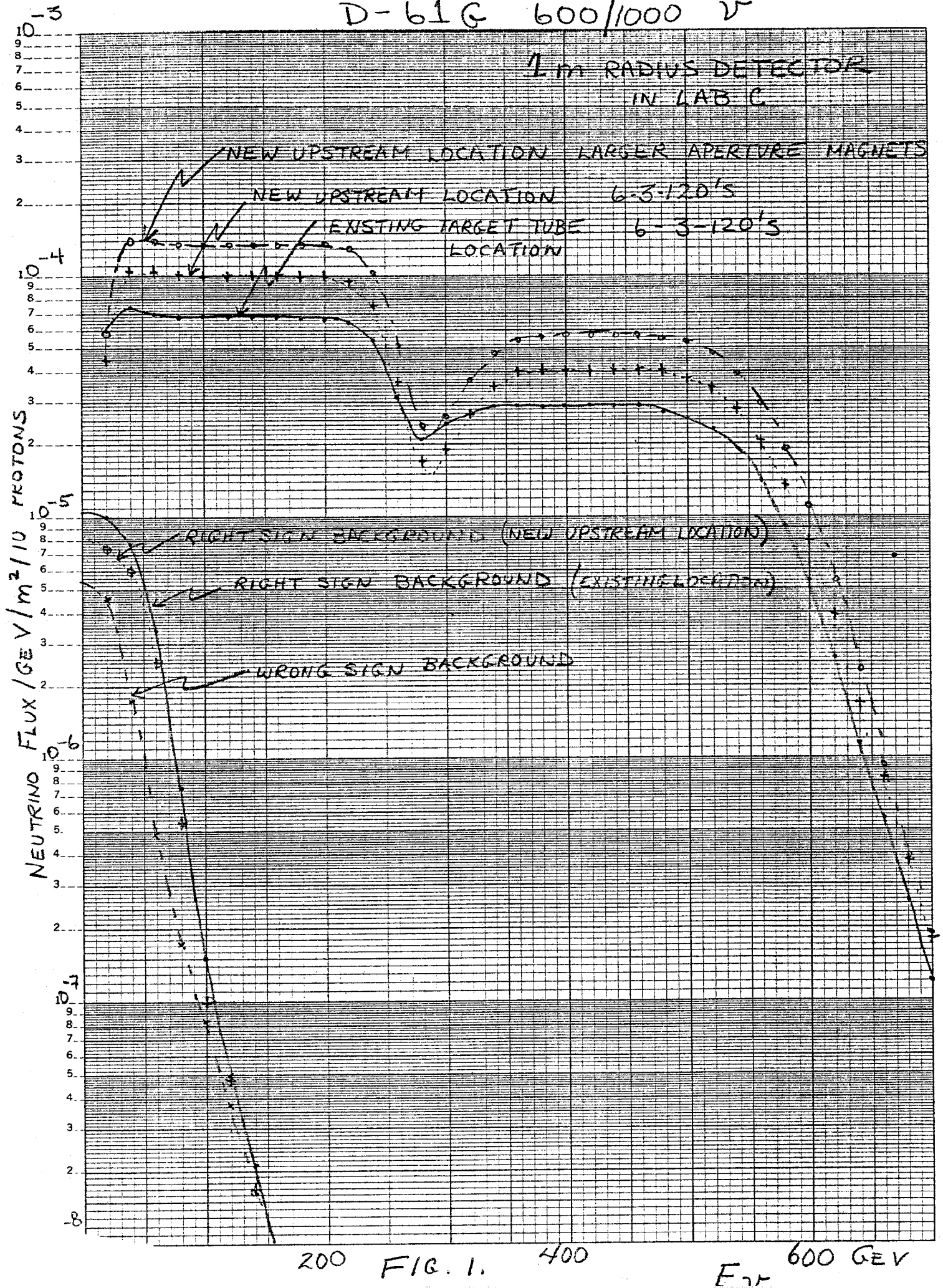
1. D.Theriot, private communication.
2. Plot is by T.Kondo for this train at 600 GeV.
3. R.Stefanski and H.White, "Neutrino Flux Distributions", FN-292, 1976.
4. K.L.Brown and Ch.Iselin, DECAY TURTLE, PM0031, 1974.

Figure Captions

1. Neutrino Flux estimates for D-61G tuned to 600 GeV secondaries at a 1 meter radius detector in the vicinity of Lab C. Three separate curves are shown: 1) D-61G as presented in TM-841, 2) D-61G moved to a new target location (about 500' upstream of the current neutrino production target and 3) D-61G at this new location and with increased aperture magnets for the final quads and bends.
2. Neutrino energy spectrum as a function of detector radius for a detector in the vicinity of Lab C. (D-61G, upstream location, large aperture magnets, 600 GeV tune.) Note that the actual number of neutrinos from  $\pi$  decay (lower energy band) is suppressed by  $\sim 10$  relative to those from K decay (higher energy band) in this scatter plot. Figure 2A is for a flat production spectrum 2B incorporates the S-W production model.
3. Prediction of a Cerenkov pressure curve obtainable from this train at a secondary tune of 600 GeV. The curve assumes an iris opening of 0.50mr with an inner blocking plug of 0.45 mr. (Curve due to T.Kondo).

D-61G 600/1000 v

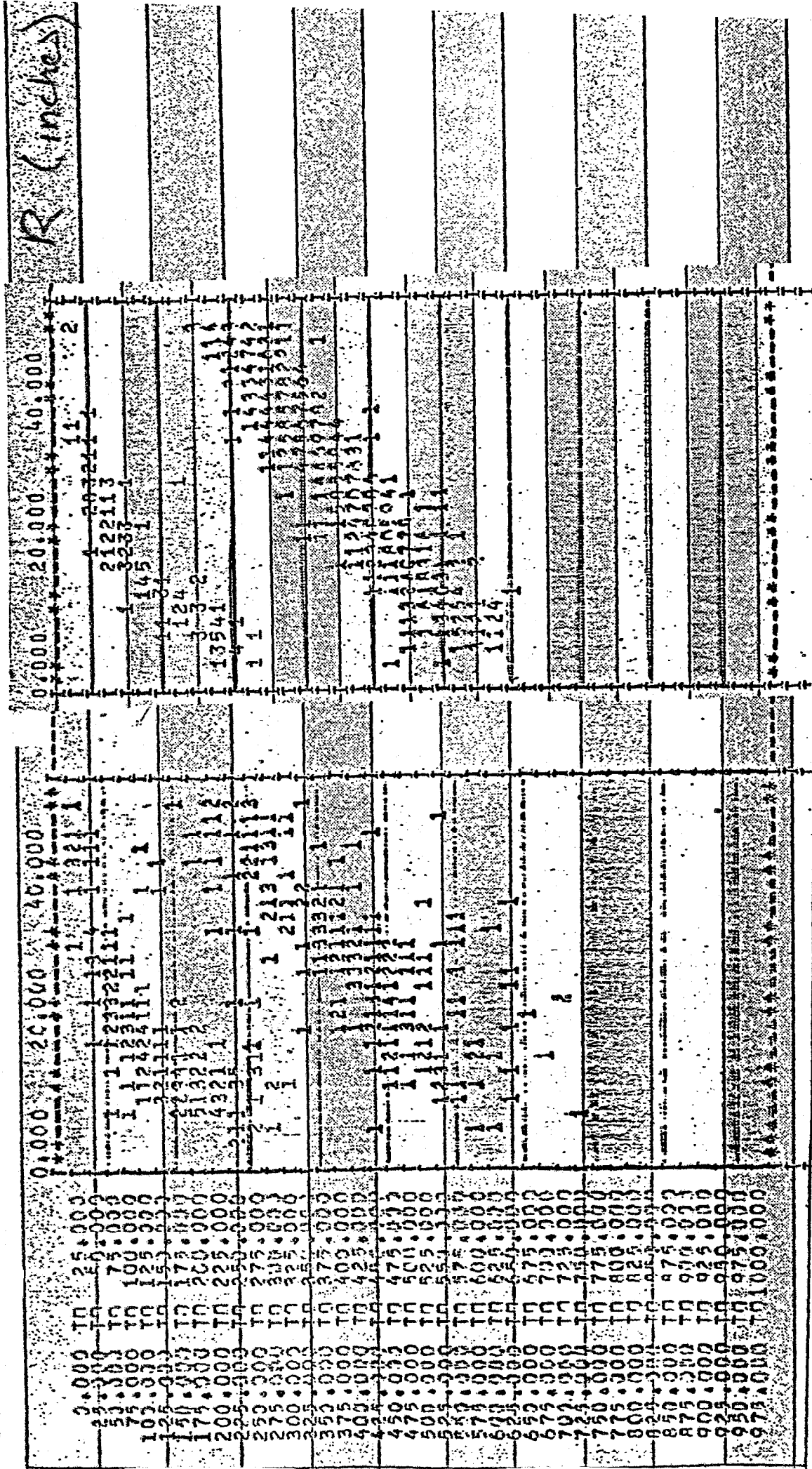
1 m RADIUS DETECTOR  
IN LAB C



HISTOGRAM NO. 2  
HORIZONTAL AXIS  
VERTICAL AXIS

R IN IN  
R IN GEV  
FOR RAYS  
FOR RAYS

5298.500 FT  
5299.500 FT  
FROM THE TARGET  
FROM THE TARGET



$P_u$  GeV

600 GeV D-61G

Flat production  
spectrum

S-W production  
spectrum

FIG 2A

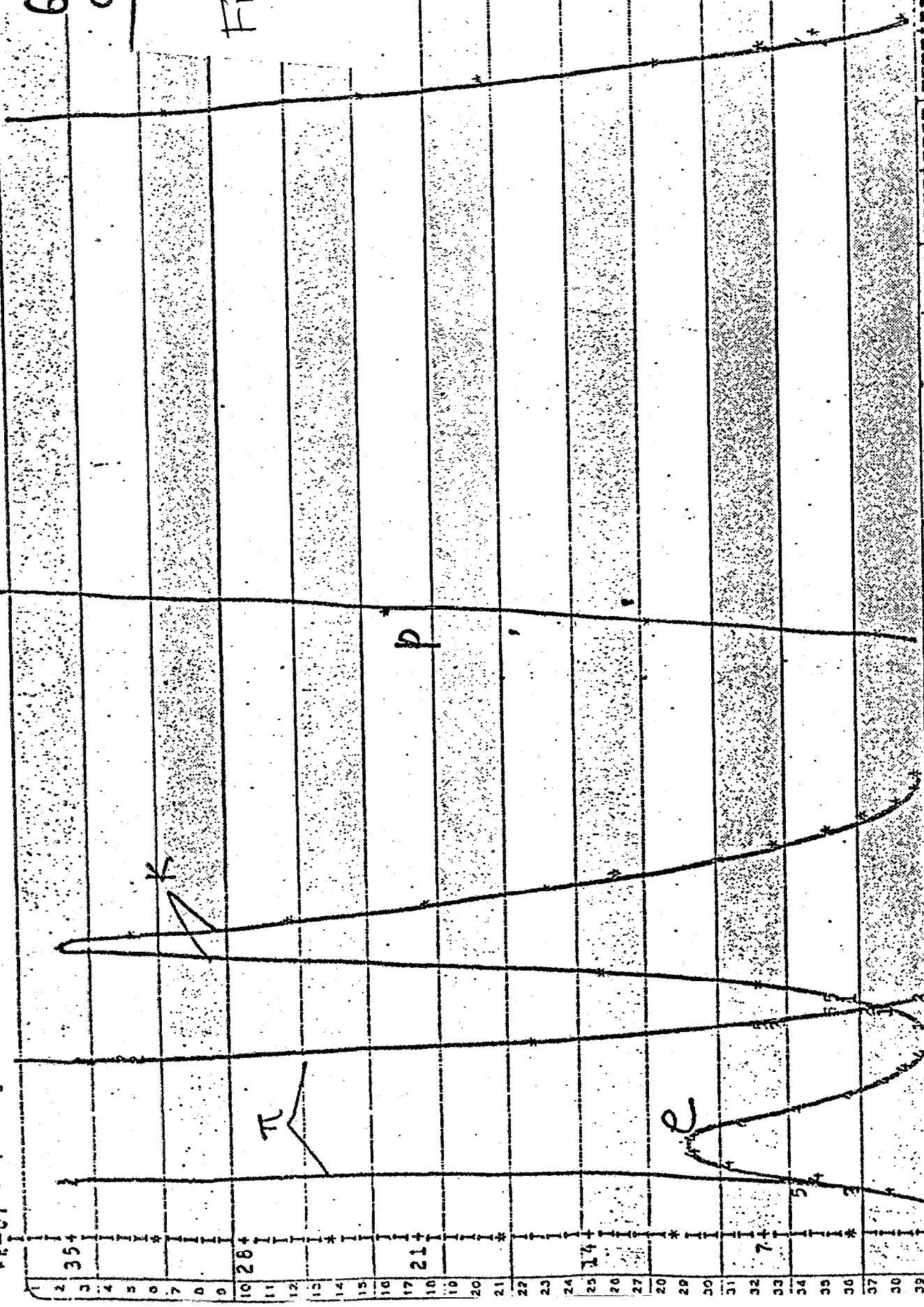
FIG 2B



11) HS= 13 KALON, OBSERVED  
 11) HS= 13 PROTON, OBSERVED  
 11) HS= 15 TOTAL= 10 + 5 DIVIDK + PROTONS  
 11) HS= 15  
 11) HS= 15  
 11) HS= 15

600 GeV  
 0.45/0.5

FIG. 3



	0.000	5.000	10.000	15.000	20.000	25.000	30.000	35.000	40.000	45.000
(HST) NO DATA	13	14	15	16	17	18	19	20	21	22
SUM	2.183E-03	1.586E-03	1.673E-03	1.673E-03	1.673E-03	1.673E-03	1.673E-03	1.673E-03	1.673E-03	1.673E-03
AVERAGE	1.673E-03	1.673E-03	1.673E-03	1.673E-03	1.673E-03	1.673E-03	1.673E-03	1.673E-03	1.673E-03	1.673E-03
STANDARD DEVIATION	1.673E-03	1.673E-03	1.673E-03	1.673E-03	1.673E-03	1.673E-03	1.673E-03	1.673E-03	1.673E-03	1.673E-03
DATA	13	14	15	16	17	18	19	20	21	22
SUM	2.183E-03	1.586E-03	1.673E-03	1.673E-03	1.673E-03	1.673E-03	1.673E-03	1.673E-03	1.673E-03	1.673E-03
AVERAGE	1.673E-03	1.673E-03	1.673E-03	1.673E-03	1.673E-03	1.673E-03	1.673E-03	1.673E-03	1.673E-03	1.673E-03
STANDARD DEVIATION	1.673E-03	1.673E-03	1.673E-03	1.673E-03	1.673E-03	1.673E-03	1.673E-03	1.673E-03	1.673E-03	1.673E-03
DATA	13	14	15	16	17	18	19	20	21	22
SUM	2.183E-03	1.586E-03	1.673E-03	1.673E-03	1.673E-03	1.673E-03	1.673E-03	1.673E-03	1.673E-03	1.673E-03
AVERAGE	1.673E-03	1.673E-03	1.673E-03	1.673E-03	1.673E-03	1.673E-03	1.673E-03	1.673E-03	1.673E-03	1.673E-03
STANDARD DEVIATION	1.673E-03	1.673E-03	1.673E-03	1.673E-03	1.673E-03	1.673E-03	1.673E-03	1.673E-03	1.673E-03	1.673E-03
DATA	13	14	15	16	17	18	19	20	21	22